Adaptive Neuron

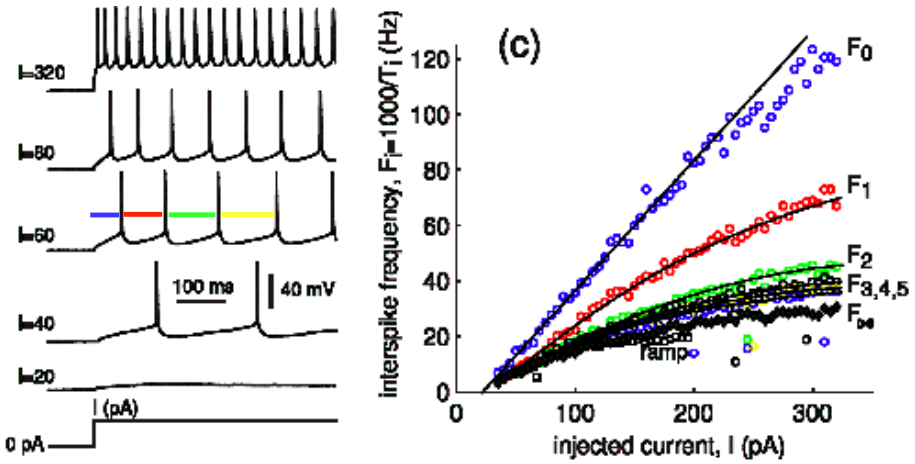

Interspike intervals (T_i) get longer and frequency drops (F_i) (rat L5 pyramidal cell) [Izhikevich07].

Adaptation has a divisive effect on $F(I)$-curve (F_∞ vs F_0 curve)

Requires an outward current that is proportional to spike rate

Model's V_m traces and $F(I)$ curves

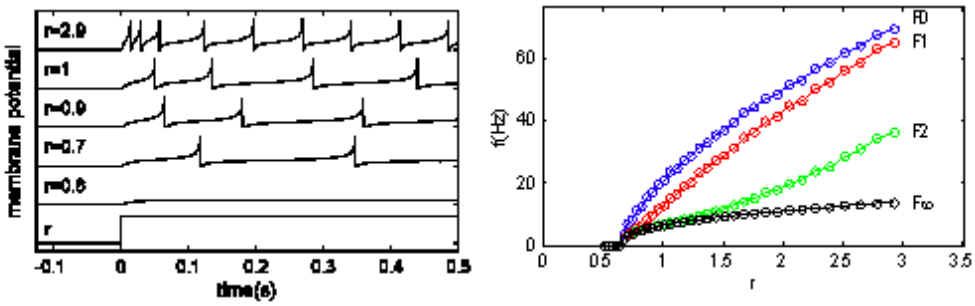

Interspike intervals lengthen (left) and sensitivity decreases (right).

This simple model displays behavior qualitatively similar to the cortical cell.

We use it to explore the role of the M-current—a slow, voltage-dependent potassium conductance.

Membrane-voltage equation

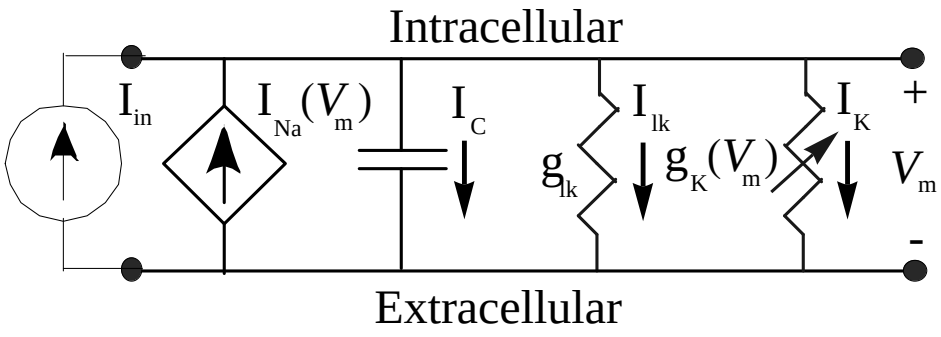

Adaptation can arise from a voltage-dependent K^+-conductance (M-current, I_K).

We add a conductance g_K in parallel with the leak:

$$C_m \frac{dV_m}{dt} + g_{lk} V_m + g_K[V_m, t] V_m = I_{in} + \frac{1}{3}\left(\frac{V_m}{V_{th}}\right)^2 g_{lk} V_m$$

This K^+-channel has a high threshold (-44mV) and therefore turns on only during a spike; it decays between spikes. In dimensionless units, we have:

$$\tau_m \frac{dx}{dt} + (1+g)\, x = r + \frac{1}{3} x^3 \quad \text{where} \quad \tau_m = \frac{C_m}{g_{lk}},\ x = \frac{V_m}{V_{th}},\ r = \frac{I_{in}}{g_{lk} V_{th}},\ g = \frac{g_K}{g_{lk}}$$

M-Current model (g_K)

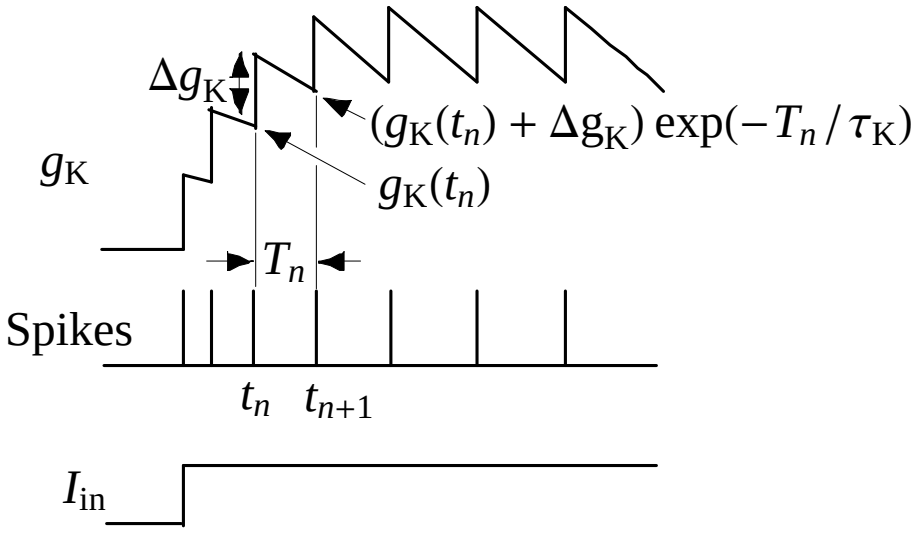

Each spike increases g_K by Δg_K; g_K decreases exponentially between spikes.

If τ_K is the K^+-channel's time-constant, we have

$$g_K[t - t_n] = (g_K[t_n] + \Delta g_K)\, e^{-(t-t_n)/\tau_K} \quad \text{for} \quad t_n < t < t_{n+1}$$

where $g_K(t_n)$ is the value just before the n^{th} spike occurs.

The net change in g_K from spike to spike is:

$$\begin{aligned} g_K[t_{n+1}] - g_K[t_n] &= (g_K[t_n] + \Delta g_K)\, e^{-T_n/\tau_K} - g_K[t_n] \\ &= \Delta g_K\, e^{-T_n/\tau_K} - g_K[t_n]\,\left(1 - e^{-T_n/\tau_K}\right) \end{aligned}$$

where $T_n \equiv t_{n+1} - t_n$ is the interspike interval. Setting $g_K[t_{n+1}] = g_K[t_n]$ and solving for $g_K[t_n]$ yields the steady-state value for this particular interspike interval:

$$g_{K\infty}[T_n] = \frac{e^{-T_n/\tau_K}}{1 - e^{-T_n/\tau_K}}\,\Delta g_K$$

M-current dynamics

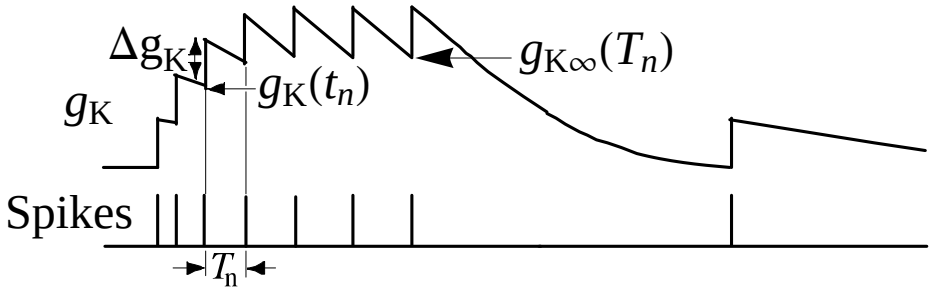

When the interspike interval stops changing, $g_K(t_n)$ reaches its steady-state value ($g_{K\infty}(T_n)$).

Rewriting our original equation

$$g_K[t_{n+1}] - g_K[t_n] = \Delta g_K\, e^{-T_n/\tau_K} - g_K[t_n]\,\left(1 - e^{-T_n/\tau_K}\right)$$

in terms of the steady-state value

$$g_K[t_{n+1}] - g_K[t_n] = (g_{K\infty}[T_n] - g_K[t_n])\,\left(1 - e^{-T_n/\tau_K}\right)$$

shows that this is a stable point: g_K rises if it is smaller than $g_{K\infty}(T_n)$, falls if it is greater, and remains unchanged if it is equal.

Nullclines

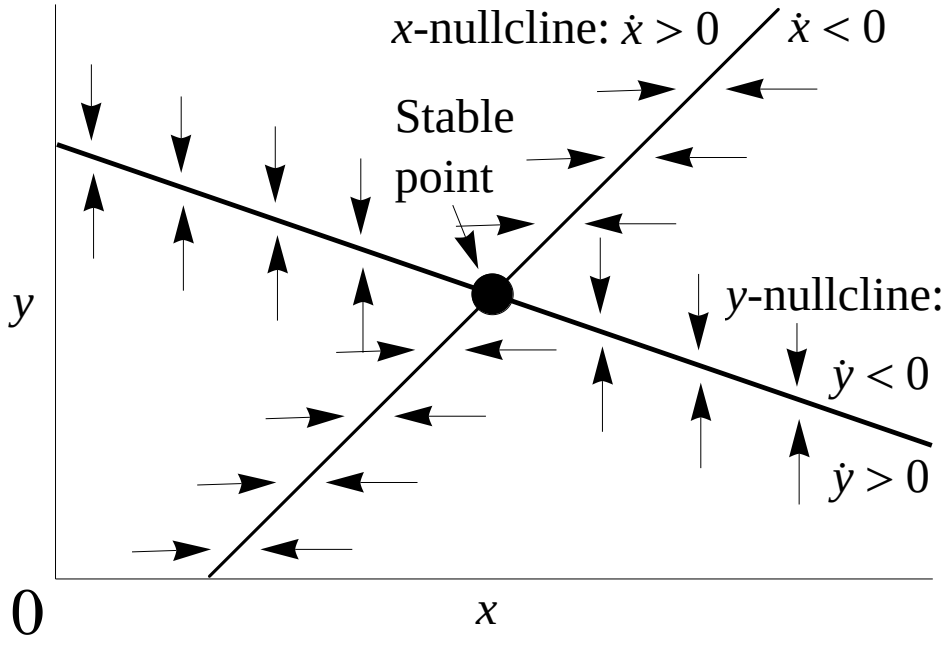

A variable's derivative is zero along its nullcline—it has opposite signs on either side of this line.

Models with two variables — two-dimensional systems — have the form:

$$\frac{dx}{dt} = g[x, y]$$
$$\frac{dy}{dt} = h[x, y]$$

Setting these derivatives equal to zero yields two relationships that define the system's *nullclines* (curve in *x*-*y* plane):

`g[x, y] = 0` *x*–nullcline
`h[x, y] = 0` *y*–nullcline

Plotting the nullclines helps us visualize the system' s dynamics:

1. Fixed points lie at the nullclines' intersection — because both derivatives are zero there.

2. Trajectories move right when left of and move left when right of the *x*-nullcline — or vise versa — because the *x*-derivative changes sign.

3. Trajectories move up when below and move down when above the *y*-nullcline — or vise versa — because the *y*-derivative changes sign.

g_K-nullcline

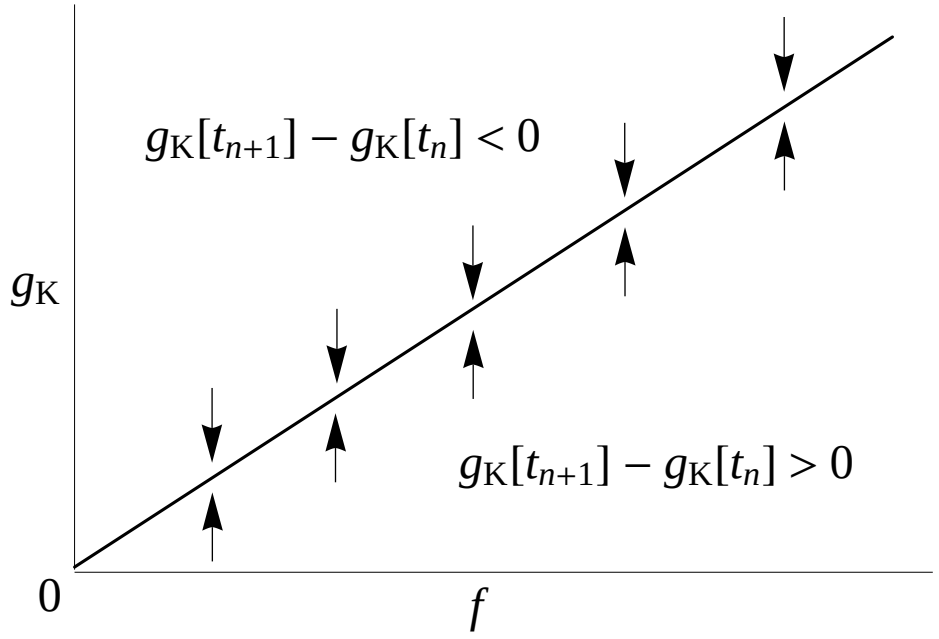

g_K's steady-state value vs spike frequency f: increases (↑) if it's smaller; decreases (↓) if it's greater.

We obtain a plot of $g_{K\infty}$ versus frequency from our expression for $g_{K\infty}(T_n)$:

$$g_{K\infty}[T_n] = \frac{e^{-T_n/\tau_K}}{1 - e^{-T_n/\tau_K}} \Delta g_K = \frac{1}{e^{T_n/\tau_K} - 1} \Delta g_K \approx \frac{\tau_K}{T_n} \Delta g_K$$

making the approximation $e^{\epsilon} \approx 1 + \epsilon$ for $\epsilon \ll 1$. With $f_n = 1/T_n$, this yields

$$g_{K\infty}[f_n] = \Delta g_K \tau_K f_n$$

f-nullcline

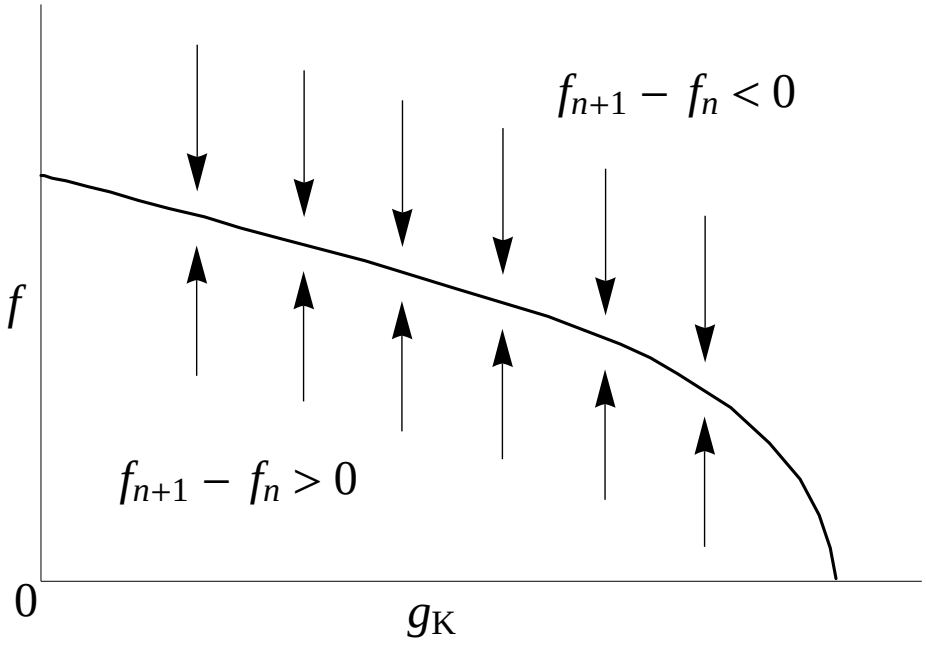

Spike frequency f for a given value of g_K.

While the neuron's spike rate f determines K-conductance's steady-state value (i.e., $g_{K\infty}(f)$), the potassium conductance in turn determines the neuron's steady-state spike rate ((i.e., $f_\infty(g_K)$). We obtain the latter relationship as before, accounting for the leak and potassium conductances with a subtractive term:

$$f_\infty[r, g] \approx \frac{3^{7/6}}{2\pi\tau_m}\left(r^{2/3} - \frac{1+g}{2}\right) \text{ where } \tau_m = \frac{C_m}{g_{lk}},\ r = \frac{I_{in}}{g_{lk} V_{th}},\ g = \frac{g_K}{g_{lk}}$$

The coefficient 1/2 was determined empirically.

Phase diagram

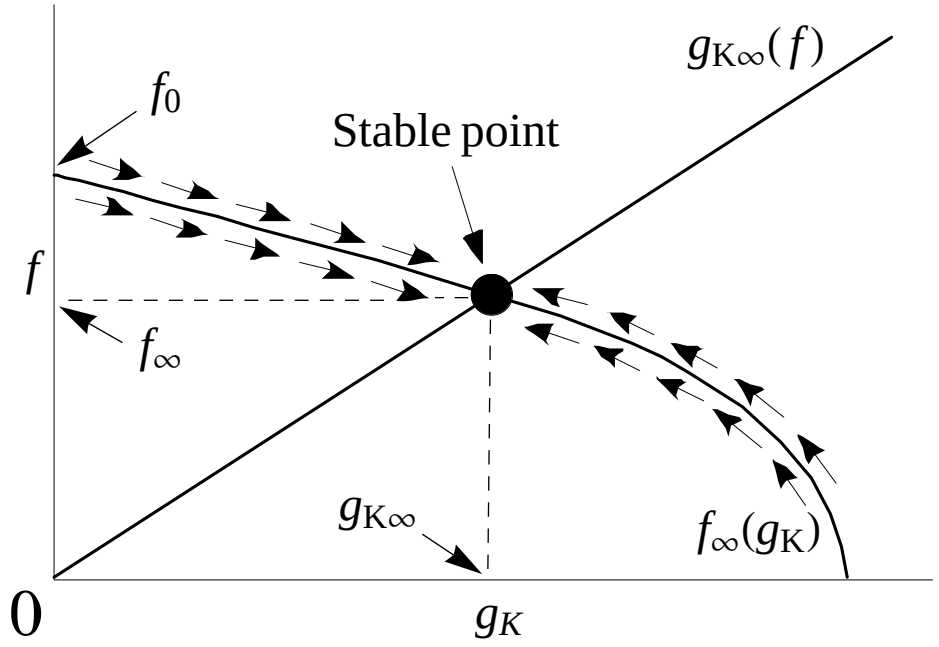

The two nullclines' intersect at a stable point. f_0 is the firing rate without adaptation.

We can assume that the f responds to changes in g_K much faster than g_K responds to changes in f. In that case, the trajectory reaches the f -nullcline quickly, and then moves along it to the g_K-nullcine slowly (i.e., $f = f_\infty(r, g)$). With g_K initially zero, the frequency starts at f_0 and decreases as g_K increases (adaptation).

Eventually, g_K reaches it's steady-state value as well (i.e., $g_K = g_{K\infty}(f_\infty)$). Normalizing this value for g_K (i.e., $g_{K\infty}(f_\infty) = \Delta g_K\, \tau_K\, f_\infty$) by g_{lk} and substituting into our expression for $f_\infty(r, g)$ yields the steady-state solution:

$$f_\infty = \frac{a}{\tau_m}\left(r^{2/3} - \frac{1 + \Delta g_K\, \tau_K\, f_\infty / g_{lk}}{2}\right) \quad \text{where} \quad a = \frac{3^{7/6}}{2\pi} = 0.573$$

$$= f_0 - \frac{a}{\tau_m}\frac{\Delta g_K\, \tau_K\, f_\infty / g_{lk}}{2} \quad \text{where} \quad f_0 \equiv f_\infty[r, 0] = \frac{a}{\tau_m}\left(r^{2/3} - \frac{1}{2}\right)$$

Solving for f_∞ yields

$$f_\infty = \frac{f_0}{1 + \frac{a}{2}\,(\Delta g_K / g_{lk})\,(\tau_K / \tau_m)}$$

Notice that adaptation has a *divisive* effect on firing rate.

How good are our approximations?

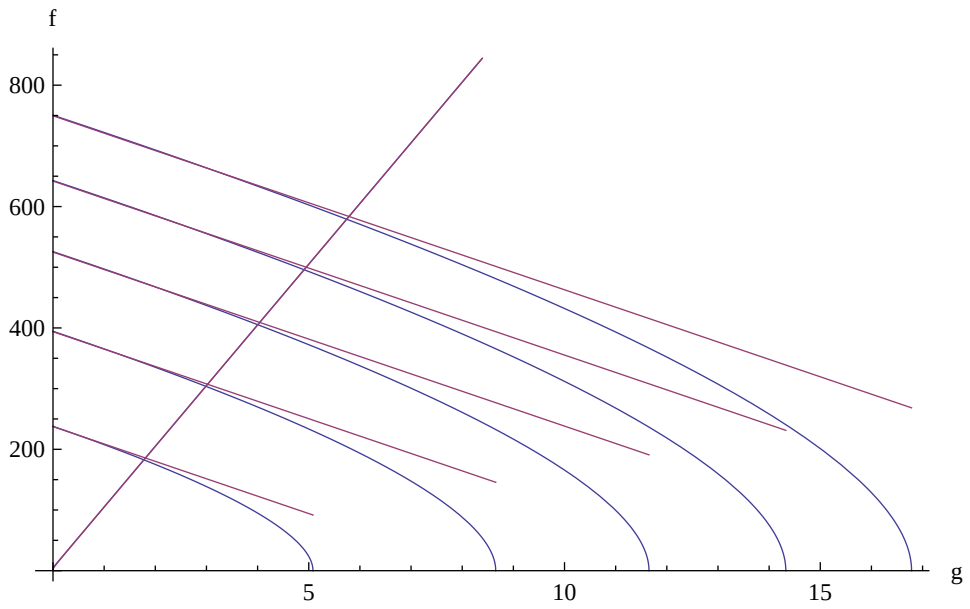

Exact $f_\infty(g_K)$ and $g_{K\infty}(f)$ expressions (blue) and their linear approximations (red) for $r = 10, 20, \ldots, 50$; g_K is normalized by g_{lk}. $g_{K\infty}(f)$'s approximation is excellent; $f_\infty(r, g)$'s is good for high firing rates. The parameter values were:

$$\left\{\tau_m \to 10\ \text{ms},\ \tau_k \to 100\ \text{ms},\ \frac{\Delta g_k}{g_{lk}} \to 0.1\right\}$$

11 of 12

Adapted firing rate (F_∞)

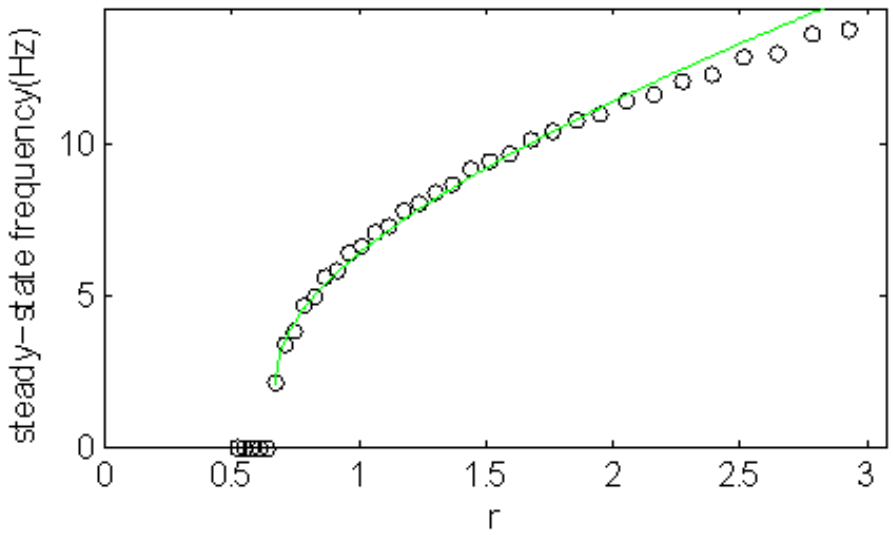

The theory (green) holds for moderate currents (a few times the minimum)

The analysis predicts that the adapted firing-rate versus current curve ($f_\infty(r)$) should only differ by the unadapted case ($f_0(r)$) by a scale factor:

$$f_\infty = \frac{f_0}{1 + \frac{a}{2}\,(\Delta g_K / g_{lk})\,(\tau_K / \tau_m)}$$

This appears to be the case.

Next Lecture: Bursting

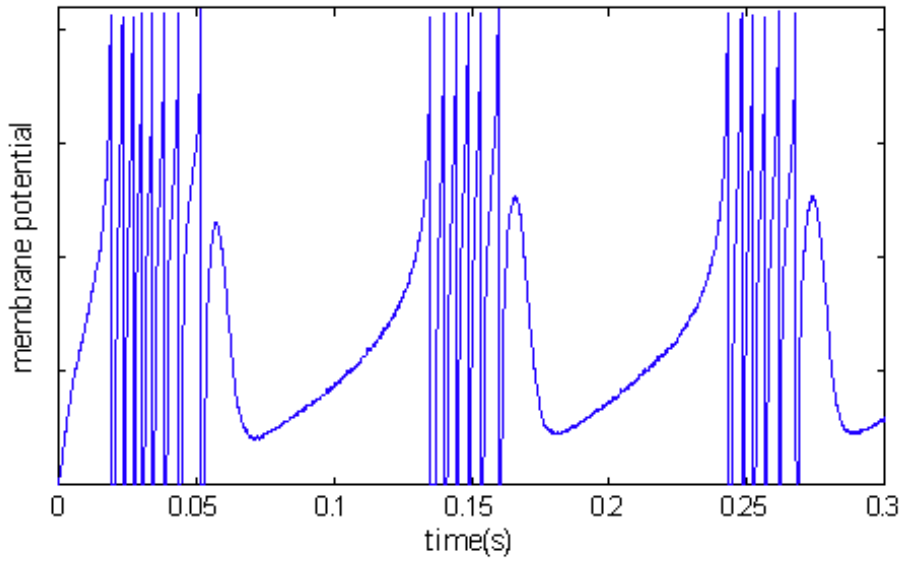

Adding a Ca^{2+} current leads to bursting.

Unlike adaptation, which requires an outward current that is proportional to spike rate, bursting requires an *inward* current that is proportional to spike rate.